Low-Intensity Ultrasound Inhibits the Long-Term Migration of Cancer Cells

Itziar González (iciar.gonzalez@csic.es)
Consejo Superior de Investigaciones Científicas CSIC

Jon Luzuriaga
University of the Basque Country (UPV/EHU)

Alba Valdivieso
Consejo Superior de Investigaciones Científicas CSIC

Jesús Frutos
Ramón y Cajal Health Research Institute (IRYCIS)

Jaime López
Consejo Superior de Investigaciones Científicas CSIC

Luis Hernández
Consejo Superior de Investigaciones Científicas CSIC

Luis Rodríguez-Lorenzo
Institute of Science and Technology of Polymers ICTP, CSIC

Virginia Yagüe
Universidad Politécnica de Madrid UPM, Escuela Técnica Superior de Ingenieros de Telecomunicación

Jose Luis Blanco
Universidad Politécnica de Madrid UPM, Escuela Técnica Superior de Ingenieros de Telecomunicación

Alberto Pinto
Consejo Superior de Investigaciones Científicas CSIC

Julie Earl
Ramón y Cajal Health Research Institute (IRYCIS)

Research Article

Keywords: cell migration, cancer cells, ultrasound, cell jamming, LICU

Posted Date: October 15th, 2021

DOI: https://doi.org/10.21203/rs.3.rs-957445/v1

Abstract

In recent years, it has been verified that collective cell migration is a fundamental step in tumor spreading and metastatic processes. In this paper, we demonstrate for the first time how low-intensity ultrasound produces long-term inhibition of collective migration of epithelial cancer cells in wound healing processes. In particular, we show how pancreatic tumor cells, PANC-1, grown as monolayers in vitro respond to these waves at frequencies close to 1 MHz and low intensities (<100 mW cm^{-2}) for 48-72 hours of culture after ultrasound irradiation. This new strategy opens a new line of action to block the spread of malignant cells in cancer processes. Despite relevant spatial variations of the acoustic pressure amplitude induced in the assay, the cells behave as a whole, showing a collective dynamic response to acoustic performance, agreeing with the “cell jamming” effect defined before in the literature. Experiments carried out with samples without previous starving showed remarkable effects of the LICUs from the first hours of culture, more prominent than those with experiments with monolayers subjected to fasting prior to the experiments. This new strategy to control cell migration opens a new line of action *in vivo* to block the spread of malignant cells.

Introduction

Collective cell migration plays a crucial role in pathological processes such as cancer invasion and metastasis, phenomena that depend on the invasive and migratory capacity of malignant cells1–6. During collective migration, cells move as a group maintaining cell-cell junctions, except for some leader cells at the front, which drive migration by scanning the environment to identify a path, while follower cells contribute to optimizing collective movement7–8. Microfluidic platforms have made it possible to observe and analyze these processes of cell migration through tissues. *In vitro* experiments show that epithelial leader cells at the edge of a wound undergo longer elongations than other cells on the front edge of the epithelial monolayer that propagate perpendicular to the direction of migration9-13. The mechanical role of leader cells during collective cell migration and some roles of mechanical forces and cell coupling in collective cell rearrangement and migration *in vitro* systems have been recently analyzed11-14.

Traction force measurements have been used to analyze epithelial wound closure in some studies in the literature15. While a wound closes, cells exhibit two types of traction force: forces pointing away from the gap, as classically observed during cell migration, and forces pointing toward the gap. Interestingly, these forces can be attributed to lamellipodial protrusions and actomyosin cable contraction. At late stages of wound closure, traction forces mostly point toward the gap. Analyses of these forces within the migratory cell monolayers show accumulation of intercellular stress from the edge to the inside of the monolayer, which induces a greater tension in the cell-cell junctions16,17. Thus, migratory cell monolayers can be seen as tissues under tension.

Other recent studies have shown surprising oscillatory movements of epithelial cells in monolayers18-20. These oscillations define movements of the cells toward the exterior of the epithelial monolayer, which

alternate with movements toward the interior in the radial direction. The unexpected variety of cell movement is related to the complex mechanical behavior of biological tissues (cells can deform) and their active nature nature21 (cells can modify their contractility or adhesive properties).

On the other hand, cell density is also an important regulator of collective cell dynamics22-24. The average cell velocity stabilizes when confluence is reached and decreases when cell density increases, leading to a switch from a fluid-like to a more solid-like state19. As cell density increases, each cell within the population becomes increasingly trapped by its neighbors, leading to reduced motion and greater correlation of motion (larger clusters of cells that migrate together). This is known as the “cell jamming” effect25. The large-scale coordination is also reduced with a rise in cell density, associated with shorter cell displacements.

Recent literature has shown that collective cell behaviors can be altered by the application of external forces, including gravity21 and chemical and physical stimuli3. The inhibitory effects of electromagnetic fields on cell monolayers have been recently analyzed26,27. However, the effects generated by oscillatory mechanical forces applied to cancer cell monolayers have not yet been analyzed in the collective migration processes of tumor cells and are discussed in this paper.

Herein, we demonstrate how low-intensity ultrasound produces long-term inhibition of collective migration of epithelial cancer cells.

Methods

Experimental Section. Conventional tissue culture assays, ultrasound generators, incubators with CO_2 supply and imaging equipment have been used for experiments on cell monolayers actuated by ultrasonic transducers. Scratched monolayers of the confluent pancreatic cell line Panc-1 were selected as samples to analyze wound healing processes with and without previous ultrasound irradiation.

Procedure. (i) Cell culture preparation, (ii) scratch-making, (iii) application of ultrasounds, iv) image filming and data acquisition, and (iv) data analysis. After exposure to different time intervals of 10, 20 and 30 min of ultrasonic treatment, the culture samples were filmed for 48 or 72 hours, depending on the experiments.

Conventional 8-well plates with rectangular geometry and flat bottom are ultrasonically driven from a piezoelectric ceramic PZ26 (Ferroperm) of a rectangular area (30 mm x 15 mm x 1.5 mm). A 10 V peak-to-peak electrical signal is supplied to the transducer at a frequency of 1 MHz, generating a continuous sine wave. The transducer is attached underneath one well containing the scratched monolayer for the transmission of vibrations. The well was exposed to acoustic intensity levels close to 60 mWatt/cm^2 (significantly lower than a tissue injury threshold described in the literature) for times of 10 min or 20 min in different experiments.

The imaging equipment consists of a bright-field microscope (Smart Cell Imager Paula of Leica Microsystems) equipped with a digital camera running its specific software for the acquisition and control of images/video during the entire culture process (Figure 1.a). Thus, the dynamics of the cells are monitored in real time after their exposure to the LICUs every 10 minutes for long periods of 24, 48 or 72 hours in different experiments. NIH Science ImageJ freeware was used to process the filmed images, allowing reconstruction of the single-cell trajectories (https://image.net/software/imagej/, University of Wisconsin-Madison).

Cell culture. The PANC-1 is an epithelioid carcinoma cell line derived from the human pancreas (Deer et al., 2010) and forms part of the ATCC human cell culture collection (https://www.atcc.org/). Standard cell culture protocols for PANC-1 cell lines were applied for cell sample preparation (E Leeper, 2009). PANC-1 cell lines were cultured in RPMI (Gibco/Invitrogen) supplemented with 10% fetal bovine serum (FBS; Invitrogen) and 50 units/mL penicillin/streptomycin (Invitrogen) and kept in an incubator at 5% CO_2 and 37°C.

Wound healing assay. Approximately 8.8x106 PANC-1 cells were plated in 8-well plates and cultured until confluent monolayers were formed. Then, the cells were either starved in serum-reduced medium (1% serum) for 24 hours (starving condition) or maintained in common complete medium (10% serum) (control). The scratches were made by using 10-µl pipette tips with a diameter of approximately 2 mm. During the wound-healing experiments, the cells were exposed to TGF-β stimulation by the addition of 1 µL of recombinant TGF-β to promote cell movement in *vitro*. The wounds were photographed at regular intervals every 10 minutes for long periods of 24, 48 or 72 hours. We determined the wound coverage of the total area and the average and standard deviation of the scratch width with the aid of the ImageJ plugin: Wound_healing_size_tool28 (WHST). The results of assays were obtained from at least three independent experiments.

We calculated the rate of cell relative wound closure according to Eq1:

$$Relative\ wound\ closure: \frac{W_i - W_f}{W_{\Delta cont}} \quad \text{(Eq1)}.$$

where W_I is the average of the initial wound area and W_f is the average of the final wound area. $W_{\Delta cont}$ refers to the substitution between the initial wound area and the final wound area of the cells cultured in control conditions, which showed higher wound closure capacity. The Alamar Blue assay was used to measure cell viability after each experiment according to the manufacturer's instructions.

Statistical Analysis. All results are presented as the mean ± standard error mean (SEM). The Mann-Whitney *U* test was performed to analyze nonparametric results. Statistical tests were performed using SPSS Statistics v.22 (IBM). Statistical significance was considered to be *$p \leq 0.05$, ** $p \leq 0.01$.

Complete analyses of cell movements/velocities were mapped and analyzed from a PIV-particle imaging velocimetry study running MATLAB, providing velocity fields of the multicell assemblies and individual

cells during wound closure, including leaders exploring the substrate and follower cells.

After application of 20 min LICUs on the monolayers, including a wound, they were cultured for 2 or 3 days and filmed every two hours (Figure 1.a). Figure 1.b shows the spatial pressure pattern established at a frequency of 1.003 MHz in a well selected for the experiments, located directly above the ultrasonic actuator. It shows bright areas that correspond to pressure nodes and dark zones to maximum pressure amplitudes of 0.29 MPa measured with a needle hydrophone (Precision Acoustics LTD, hydrophone SN 1423). Polystyrene beads with diameters of 20 µm were used to observe the 2D pressure pattern collected at the pressure nodes of the standing waves generated throughout the well. Nodes and antinodes are separated short distances of less than 1 mm. The wound made in the cell monolayer also includes multiple pressure nodes along its length in both directions, width and length of the gap.

All methods described were carried out in accordance with relevant guidelines and regulations of the host institutions. Samples from human subjects were not used in this study.

Results And Discussions

Once the cell monolayer is scratched, the wound presents sharp straight boundaries that become blurred as the healing process progresses. Thus, the healing process occurs irregularly. The rate of cell migration can be quantified using two single metrics: the *wound width* as the average distance between the edges of the scratch and/or the *wound area*, which is calculated by the cell-free area in captured images. During this process, nearby leader and follower cells migrate in different directions, not just in the direction of the width of the wound. The cells disperse, making the contours of the wound less sharp and less straight.

Cells migrate when exposed to an empty space. Under normal conditions, the wound takes approximately 1.5 days to close for Panc-1 cancer cells. Figure 2 shows the average velocities of dozens of cells near the wound boundary in a movie of our experiments. They are drawn by green arrows overimposed in the filmed images. Each cell on the leading edge has a velocity vector pointing in the direction of migration. These measurements provide information about the polarity of cell clusters and dynamic cell flows and the degree of cell-cell rearrangement. Cell movements occur at low Reynolds numbers (Stokes regime), which means that viscous drag of their surrounding medium dominates inertial movements, slowing down the cell movements. In this way, cell dynamics could be assimilated to fluid dynamics. However, cell behaviors cannot be attributed to simple laminar flows. In contrast, cells often show coordinated rotational motions that span over dozens of cells near the edges of the wound in the monolayer, including swirling movements of cell groups and vortices, also observed in these processes (rotation motion described by green arrows in the images of Figure 2)17.

The leading cells at the border of the migrating tissue adhere and migrate in amaeboid motion on the substrate through the adhesion assembly and extensions of fillopodia that propagate perpendicular to the direction of migration, as described previously in the literature9-13. In addition, other cell biological

processes could occur in parallel during collective cell migration, such as proliferation, which is limited under starving conditions. In our experiments, we found that leader cells enlarge their shapes and acquire higher velocity amplitudes than follower cells to scan the substrate free of cells, according to the literature.

However, after LICU irradiation, the leader cells acquire different unexpected behaviors, as described in the following.

Effects of LICUs on cell migration in PANC-1 monolayers. Long-term effects were observed on the cell motion. The cells do not undergo any individual or collective movement during sonication or during the following hours, but they show altered dynamics several hours later and two days after LICU treatment. Thus, this dynamic does not respond to Newtonian forces with immediate action but rather induces altered long-term dynamics during at least two days of culture after ICU treatment.

Figure 3 shows long-term trajectories described by dozens of cells bearing the faced edges of the monolayer wound. They were reconstructed in ImageJ freeware from different cells of the monolayer near the wound boundaries after 20 min irradiation of LICUs before culture.

Figure 4 shows three culture processes with different doses of ultrasonic irradiation. The healing process of the wound showed a delay dependent on the time of the LICU treatment. Figures 4.b and 4.c show different delays in wound closure after acoustic irradiation for 10 min and 20 min, respectively, with respect to the time required by the samples for wound closure (Figure 4.a). A supplementary video (Video MM1) shows a wound healing process without closure 48 hours after 20 min of ultrasonic irradiation. This inhibitory effect induced on cell migration was repeatedly observed in experiments.

On the other hand, we found that cancer cell monolayers behave as a single tissue rather than a succession of linked cells exposed to different acoustic conditions defined by their respective positions along the acoustic pressure pattern established in the chamber of treatment with high spatial variations in very short distances of quarter of wavelength between nodes and antinodes (close to 375 μm) (Figure 1.b).

Some leader cells showed complex trajectories described throughout the substrate, not only along the gap direction but also describing displacements in directions transverse to it, mainly the leader cells at the edge of a wound. Looking in detail at the motion of single cells in the wound area, erratic motion of some leader cells from faced wound edges was observed during the second day of culture after ultrasound irradiation.

A supplementary video **MM2.mp4** shows two other compared movies with overimposed colours on each cell quantifying their individual displacements, including amplitude and direction of motion. Figure 5 shows an instantaneous snapshoot of the two movies included in the video without and with LICU irradiation at the same culture time. Colors in the images refer to the direction of displacement and are

described in the figure. In particular, red refers to right-direction cell displacements, green refers to left-direction displacements, blue refers to vertical displacements and yellow refers to stagnant conditions.

The majority of cells from the left wound edge show red colors during their progression toward their faced wound edge and vice versa. However, several leader and follower cells behind the leaders experience complex reversible and rotational motions over time, showing different colors in the images. Thus, in a natural woudn helaing process, wihtout any external forcé applied, PANC-1 leader and follower cells in the first 6-8 rows behind the left edge (Figure 5.a) show large displacements toward the wound gap to find cells coming from the right edge of the gap which experience displacements in the opposed direction, coming both sets of cells together in relatively short times close to 1 day. In contrast, the cáncer cells in monolayers exposed before to 20 min-LICUs partially inhibited their motion, describing very slow displacements over long times (Supplementary video **MM2.mp4**). These samples require much longer times for wound closure, even 72 hours.

Influence of the wound width on the cell motion. Greater displacements and higher migration velocity amplitudes were found in samples with wider wound widths (Figure 5). Wider the wound, the wound closure process is faster until a certain wound width from which its closure process slows down. Figure 5.c shows the progression of five average velocity amplitudes measured from respective movies of wound healing starting from different wound widths. These graphs were obtained from five assays in which the dynamics of hundreds of cells were analyzed. In the experiments, average velocities higher than 8 μm/h were found on samples with initial wound widths close to 600 μm (graphs of Assays 2 and 4 in the figure), which decreased over time by approximately 60% until reaching a gap with widths close to 200 μms, showing a decrease of approximately 60%. Meanwhile, lower average cell velocities of narrower wounds were found in the experiments, between 2.5 and 6.0 μm/h for gaps ranging from 200-300 μm (graphs of Assays 1, 3 and 5, respectively), similar to those of wider wounds once this gap size was reached.

This slowdown in the wound closure process is associated with the approximation between the monolayer fronts, increasing cell density and decreasing the distance between cells. This finding may be indicative of a solid-state behavior of the cell monolayer rather than fluid-like behavior, often assumed in the literature22.

Attraction-repulsion processes between single leader cells. Attraction-repulsion processes were found in the experiments between pairs of leader cells separated from the opposed boundaries of the wound during part of the 2nd day of culture that was previously irradiated with 20 min LICUs (Figure 6). It is an unexpected behavior not reported before in the literature that takes almost ten hours of culture during the second day (between 26th —35th hours of culture). After 48 hours, cells A and B remained separated, and both joined back to their respective initial wound boundaries.

During their mutual attraction-repulsion process, the cells change their shape and volume in a process of dual expansion-retraction, spreading multiple fillopodia during their apparent erratic displacements

throughout the substrate. After this process, the cells do not join to remain together, but they return to their initial wound edges, leaving the wound open at the end of the period of observation.

Influence of starvation on the wound healing processes after LICU irradiation. Four different types of experiments were carried out according to the combination of two variables or conditions: LICU irradiation treatment and serum starvation for 24 h before the treatment/culture. They provided different results that were analyzed and compared in the following.

Figure 8 shows quantified results of wound progression over time for these four test conditions referred to different treatments before the sample cultures. For this analysis, wounds with initial widths of 400 μm were made on PANC-1 monolayers to start under similar physical conditions.

Relative wound closure in control samples without LICU irradiation. Monolayers previously exposed to starvation showed a value of 0.5 relative to wound closure after 24 h of culture, as shown in Fig. 7a.). In contrast, the wound of samples not starved closed much more rapidly, probably due to a combined effect of cell migration and proliferation. An increase of approximately 0.9 was found after 24 hours in control cultures under nonstarving conditions (Figure 7b). However, after 48 hours, the relative wound closure value was similar in both cases (starving and nonstarving control cells).

Wound healing processes after 20 min of LICU treatment. Again, effects in samples previously exposed to starvation were not noticeable during the first 24 hours of culture (Figures 7.a). However, differentiated quantified effects were evident in the long term at 48 hours of culture.

In contrast, samples not exposed to starvation demonstrated a notable influence of LICUs on the relative wound closure at 24 hours (Figure 7b).

Some PANC-1 cell monolayers cultured under starving conditions prior to scratching were exposed to LICUs, but others were not. The relative wound closure measure and its posterior statistical analysis demonstrated that those cells irradiated with ultrasounds did not show any difference from control cells in the first 24 hours after the wound (Figure 7a). However, the effect of LICUS seems to begin in the next 24 hours, where the relative wound closure ratio was 0.2 points lower in treated cells than in control cells. Furthermore, statistical analysis confirmed the significant difference between the two groups at 48 h, $*p \leq 0.05$. As starvation is commonly used to ensure that only migration in wound healing assays is being assessed, this experiment confirms the effect of LICUS on migration inhibition of PANC-1 cancer cells.

To verify whether LICUS affected any other event apart from migration, a nonstarving wound healing assay was carried out (Figure 7.b). Surprisingly, both relative wound closure and statistical analysis revealed the important impact of LICUS in other cellular events. In this case, the difference in relative wound closure was overwhelming since the beginning of the assay. As shown in Figure 7b, at both 24 h and 48 h, the PANC-1 cells treated with LICUS showed a much lower relative wound closure ratio than their control homologs. The relative wound closure ratio was decreased by 0.6 points in the first 24 hours and 0.5 points in the posterior 24 hours compared to nontreated cells. This was supported by statistical

analysis, which showed a **p≤0.01 in both cases. This result suggests an effect of LICUS in the inhibition of other cell events, such as proliferation or in the synergy of proliferation and migration.

Further research is necessary to elucidate which patients have been affected in this case. Regardless, as the wound closure ratio is decreased, it could be a game changer for future anticancer research, with cell proliferation and dissemination being one of the most important challenges in cancer treatment.

In summary, nonstarving cell monolayers show quantitatively remarkable effects from the first hours of culture when irradiated with ultrasound. However, the monolayers subjected to fasting prior to the experiments did not show the effects of LICUs so clearly during the first 24 h of cultivation, but rather they were manifested later, on the 2nd day, and they are not as prominent effects as those found in the experiments without starving.

Cell Viability after LICUs irradiation. Cell viability was analyzed after the experiments using Alamar BLUE assays. There was no significant change in viability in response to LIUS, as shown in Figure 8, in which data from 4 replica experiments are displayed.

Conclusion

In this paper, the effects of low-intensity ultrasound on collective cell migration were investigated. In summary, LIUs hinder the migration of epithelial cancer cells in wound healing-induced processes. In particular, we show how pancreatic tumor cells, PANC-1, grew as monolayers in vitro with a wound sense and responded to these waves at frequencies close to 1 MHz and low intensities (<100 mW cm^{-2}) for 48-72 hours after ultrasound irradiation. In particular, the wound remains open for at least 48 hours or even 72 h after short-term acoustic treatments of less than 25 min, depending on the ultrasonic dose selected.

Different wound healing processes were found depending on various parameters, such as the irradiation dose or the wound width. The effects of different sonication times (10 and 20 min) and incubation times postsonication were investigated. Both irradiation times analyzed demonstrated a significant effect on cancer cell migration inhibition after postsonication incubation times.

Despite the wide pressure amplitude spatial gradients in the small area containing the wound, the cells behave as a whole, showing a collective dynamic response to acoustic performance, a bulk-like behavior of the cell monolayers after their exposure that agrees with the “cell jamming” effect defined previously in the literature25. This is a behavior also observed in previous experiments carried out on tumor pancreatic explants treated with LICUs for longer times, up to two hours of acoustic irradiation29.

In addition, nonstarving cell monolayers showed quantitatively remarkable effects from the first hours of culture when irradiated with ultrasound, unlike monolayers subjected to fasting prior to the experiments, which did not show the effects of LICUs so clearly during the first 24 h of cultivation.

The effects of LICUs on samples without starving were more prominent than those of the monolayers presviously exposed to starvation for 24 h.

The findings from this study highlight relevant inhibitory effects of ultrasound on cell migration and probably on proliferation in tissues where fasting processes cannot be applied, such as in vivo cancer tissues. These results offer a noninvasive strategy based on low-intensity ultrasounds that opens a door for future strategies to revert/modulate tumor progression and invasion.

Declarations

Acknowledgments

We want to acknowledge the following funding related to the effects of ultrasounds on cancer cells and tissues: Spanish National Plan project RETOS DPI 2017-90147-R. Intramural call for new research projects for clinical researchers and emerging research groups. IRYCIS. (2018/0240).

Author contributions (names must be given as initials)

I.G. and J. E. made a substantial contribution to the conception and design of the study, acquiring the data and in the analysis and interpretation of the results, as well as drafting and review until the final version of the manuscript.

J. L. J. L. and A. V. contributed to the processing of images and analysis of results obtained from the experiments.

I.G. J.L., A. V. and J. E. wrote the main manuscript text.

A. V., J. F., L. H. and L. R.-L. were involved in the performance of the experiments and analysis of the results.

V. Y. and J.- L. B. contributed to the implementation of supporting algorithms, formal techniques to analyze-synthesize study data, and analysis of results obtained from the experiments.

A. P. contributed to the development of the assay to carry out the experiments.

Additional information

Supplementary video **MM1.mp4** shows two comparative movies from wound healing processes experienced by PANC-1 cell monolayers under natural conditions (without any external force applied) and after 20 min of ultrasound irradiation. A clear delay of gap closure can be observed after acoustic treatment, showing inhibition of collective cell migration.

Supplementary video **MM2.mp4** shows two other movies with overimposed colors on each cell quantifying their individual displacements, including amplitude and direction of motion.

All persons listed as authors have given their approval for submission of the paper.

The authors declare no competing interests.

References

1. Friedl, P. & Gilmour, D. Collective cell migration in morphogenesis, regeneration and cancer. Nat. Rev. Mol. Cell Biol. **10**, 445–457 (2009).
2. Yilmaz M, Christofori G. Mechanisms of motility in metastasizing cells. Mol Cancer Res. 2010 May;8(5):629-42. doi: 10.1158/1541-7786.MCR-10-0139. Epub 2010 May 11. PMID: 20460404.
3. Li, L, He, Y, Zhao, M, Jiang, J. Collective cell migration: Implications for wound healing and cancer invasion. Burns Trauma. **18,** 21-6. (2013).
4. Haeger, A., Wolf, K., Zegers, M. M. & Friedl, P. Collective cell migration: guidance principles and hierarchies. Trends Cell Biol. **25**, 556–566 (2015).
5. Scarpa, E. & Mayor, R. Collective cell migration in development. J. Cell Biol. **212**, 143–155 (2016).
6. Mayor, R. & Etienne-Manneville, S. The front and rear of collective cell migration.Nat. Rev. Mol. Cell Biol. **17**, 97–109 (2016).
7. Khalil, A. A. & Friedl, P. Determinants of leader cells in collective cell migration. *Integr. Biol.* **2**, 568–574 (2010).
8. Mayor 2016
9. Reffay, M. *et al.* Orientation and polarity in collectively migrating cell structures: statics and dynamics. Biophys. J.**100**, 2566–2575 (2011).
10. Wirtz, E. D, Konstantopoulos, K & Searson, PC. The physics of cancer: the role of physical interactions and mechanical forces in metastasis. Nat Rev Cancer **11**, 512–522 (2011).
11. Reffay, M. et al. Interplay of RhoA and mechanical forces in collective cell migration driven by leader cells. *Nat. Cell Biol.* **16**, 217–223 (2014).
12. Yamaguchi, N., Mizutani, T., Kawabata, K. & Haga, H. Leader cells regulate collective cell migration via Rac activation in the downstream signaling of integrin β1 and PI3K. Sci. Rep. **5**, 7656 (2015). https://doi.org/10.1038/srep07656
13. Trepat X., Sahai E., Mesoscale physical principles of collective cell organization, Nature Physics 2018, **14**(7), https://doi. 10.1038/s41567-018-0194-9
14. Saraswathibhatla, A., Galles, E.E. & Notbohm, J. Spatiotemporal force and motion in collective cell migration. *Sci Data* **7,** 197 (2020). https://doi.org/10.1038/s41597-020-0540-5
15. Brugues A. et al. Forces driving epithelial wound healing. Nat. Phys. **10**, 684–691 (2014)
16. Trepat, X. et al. Physical forces during collective cell migration. Nat. Phys. **5**, 426–430 (2009)

17. Vedula, S. R. K. et al. Emerging modes of collective cell migration induced by geometrical constraints. Proc. Natl Acad. Sci. USA **109**, 12974–12979 (2012)
18. Serra-Picamal, X. et al. Mechanical waves during tissue expansion. Nat. Phys. **8**, 628–634 (2012)
19. Deforet, M., Hakim, V., Yevick, H., Duclos, G. & Silberzan, P. Emergence of collective modes and tridimensional structures from epithelial confinement. Nat. Commun. **5**, 3747 (2014)
20. Notbohm, J. et al. Cellular contraction and polarization drive collective cellular motion. Biophys. J. **110**, 2729–2738 (2016)
21. Ladoux, B., Mège, RM. Mechanobiology of collective cell behaviors. *Nat Rev Mol Cell Biol* **18,** 743–757 (2017). https://doi.org/10.1038/nrm.2017.98
22. Kocgozlu, L. et al. Epithelial cell packing induces distinct modes of cell extrusions. Curr. Biol. **26**, 2942–2950 (2016)
23. Park, J. A., Atia, L., Mitchel, J. A., Fredberg, J. J. & Butler, J. P. Collective migration and cell jamming in asthma, cancer and development. J. Cell Sci. **129**, 3375–3383 (2016)
24. Garcia, S. et al. Physics of active jamming during collective cellular motion in a monolayer. Proc. Natl Acad. Sci. USA **112**, 15314–15319 (2015)
25. Sadati, M., Qazvini, N. T., Krishnan, R., Park, C. Y. & Fredberg, J. J. Collective migration and cell jamming. Differentiation **86**, 121–125 (2013)
26. Garg, A.A., Jones, T.H., Moss, S.M. *et al.* Electromagnetic fields alter the motility of metastatic breast cancer cells. *Commun Biol* **2,** 303 (2019). https://doi.org/10.1038/s42003-019-0550-z
27. Cios, A.; Ciepielak, M.; Stankiewicz, W.; Szyma ´nski, Ł. The Influence of the Extremely Low Frequency Electromagnetic Field on Clear Cell Renal Carcinoma. Int. J. Mol. Sci. 2021, **22**, 1342. https://doi.org/10.3390/ijms22031342
28. Suarez-Arnedo, A., Torres Figueroa, F., Clavijo, C., Arbeláez, P., Cruz, J. C., & Muñoz-Camargo, C. (2020). An ImageJ plugin for the high throughput image analysis of in vitro scratch wound healing assays. PloS one, 15(7), e0232565
29. Bazou D., Maimon N., Munn L, I. Gonzalez, Effects of low intensity continuous ultrasound (LICUS) on mouse pancreatic tumor explants, Applied Science 2017, **7**, 1275. https://doi. 10.3390/app7121275 2017
30. https://genome.ucsc.edu/ENCODE/protocols/cell/human/PANC-1_Myers_protocol.pdf

Figures

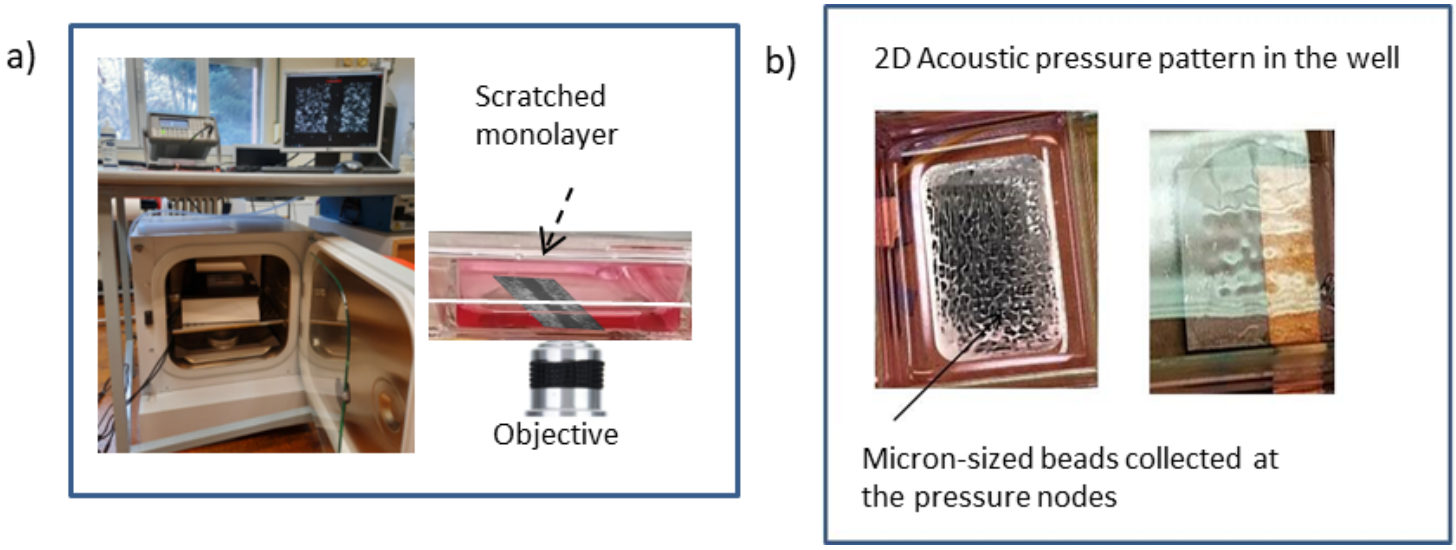

Figure 1

a) Experimental setup including the ultrasound generator, transducer, microscope inside the incubator and image processor; b) Acoustic pressure pattern established at f=1.003 MHz in the well directly located over the ultrasonic actuator. Polystyrene beads (20 μm) collect at the pressure nodes, drawing this pattern.

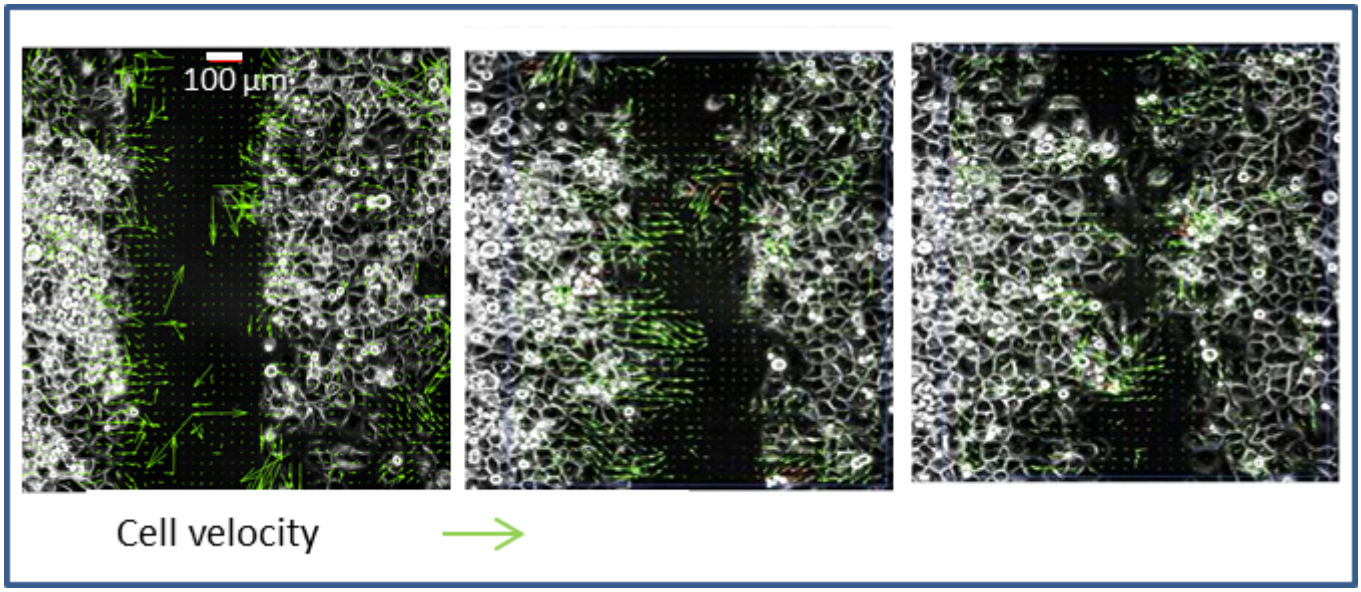

Figure 2

Distribution of PANC-1 cell velocities obtained by the PIV-MATLAB code (green arrows) overimposed on microscopic images of a wound healing process in three frames taken every 6 hours. Scale bar: 100 μm

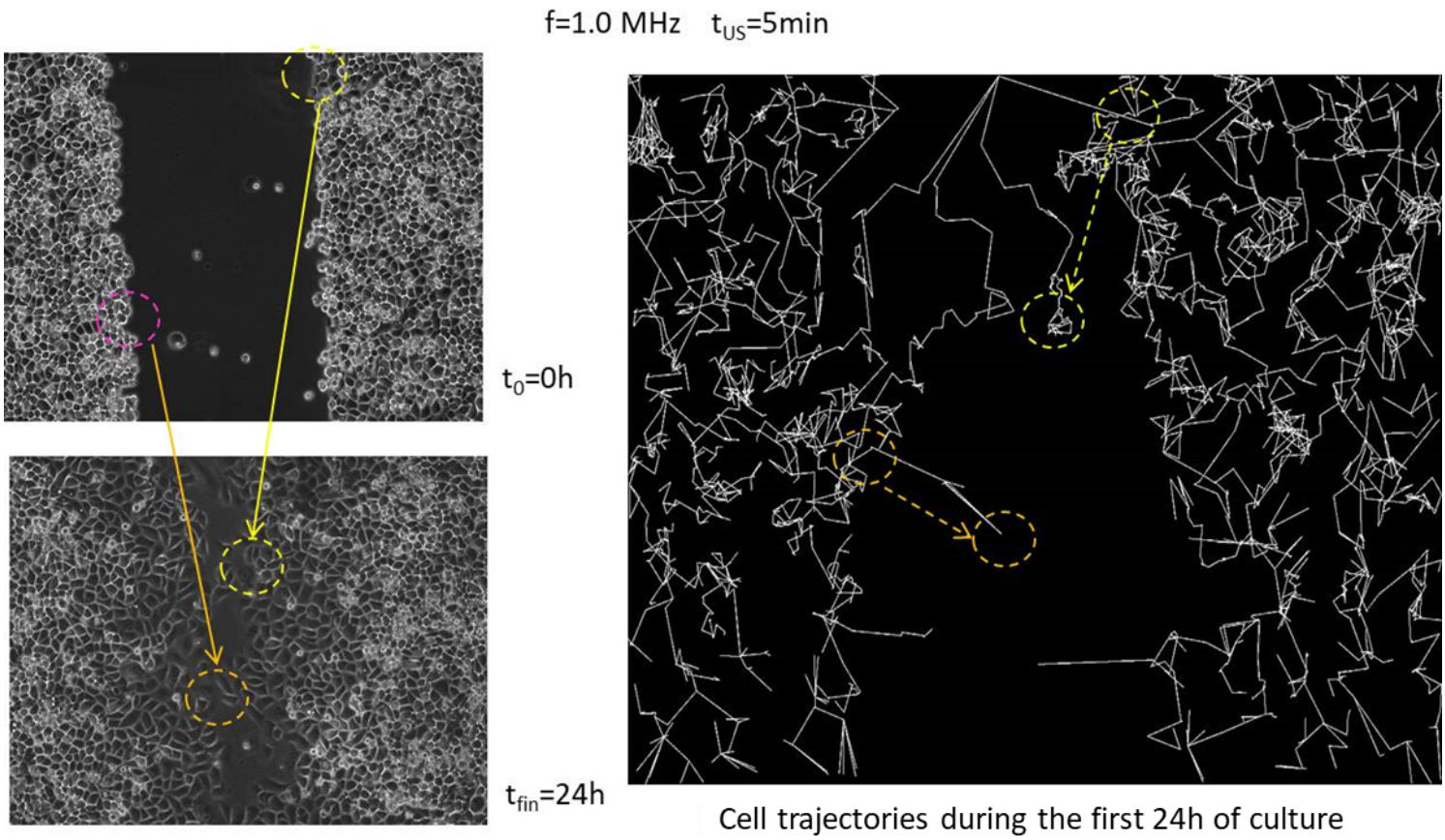

Figure 3

Cell trajectories described by cells near the wound boundaries after 20 min of irradiation of LICUs before culture.

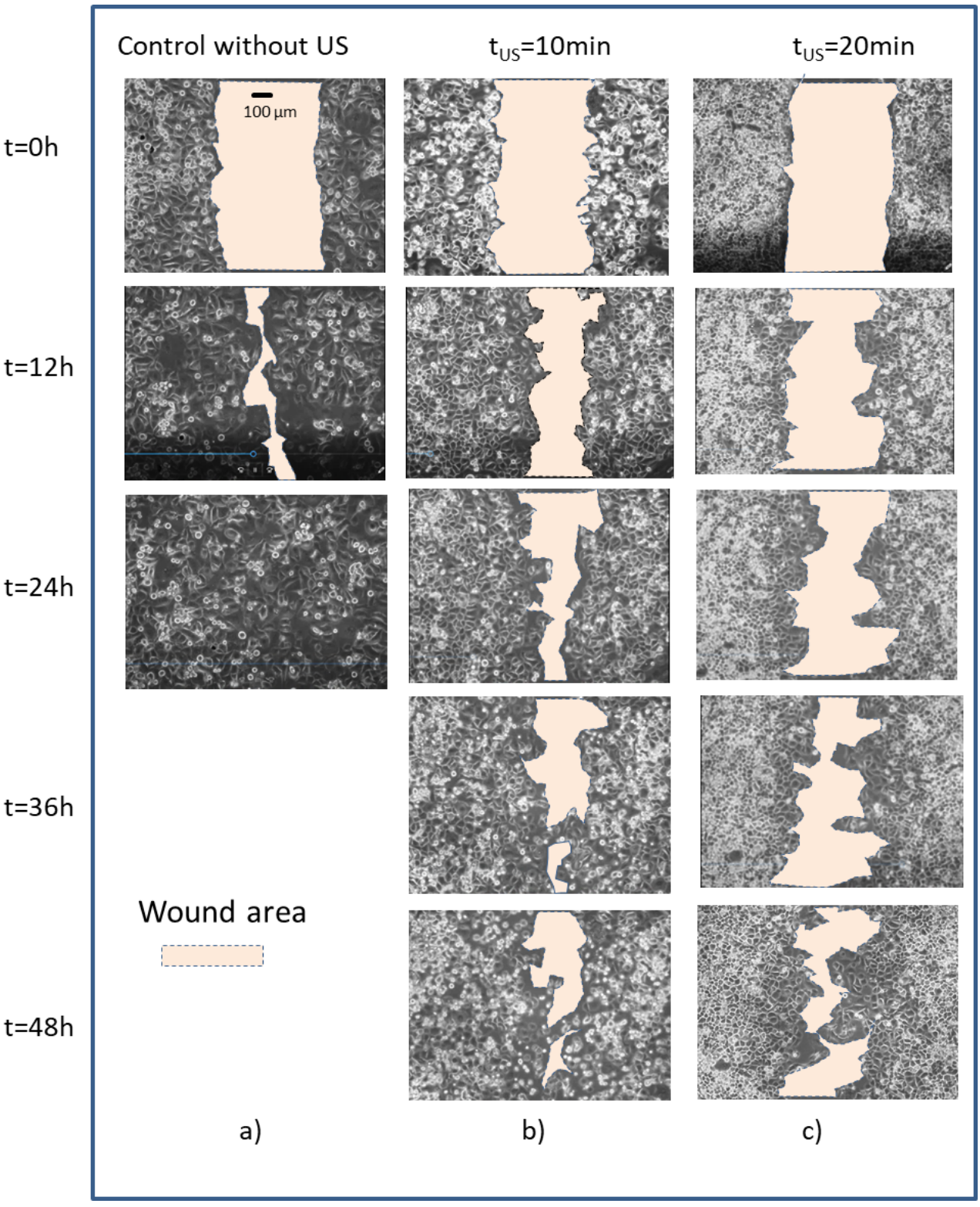

Figure 4

Filmed PANC-1 cell migration during wound healing processes: a) under normal conditions, without ultrasound irradiation; b) after exposure to LICUs at tUS=10 min; c) after LICU irradiation at t=20 min. Both sonication doses keep the wound opened for at least 48 h after the sample exposure.

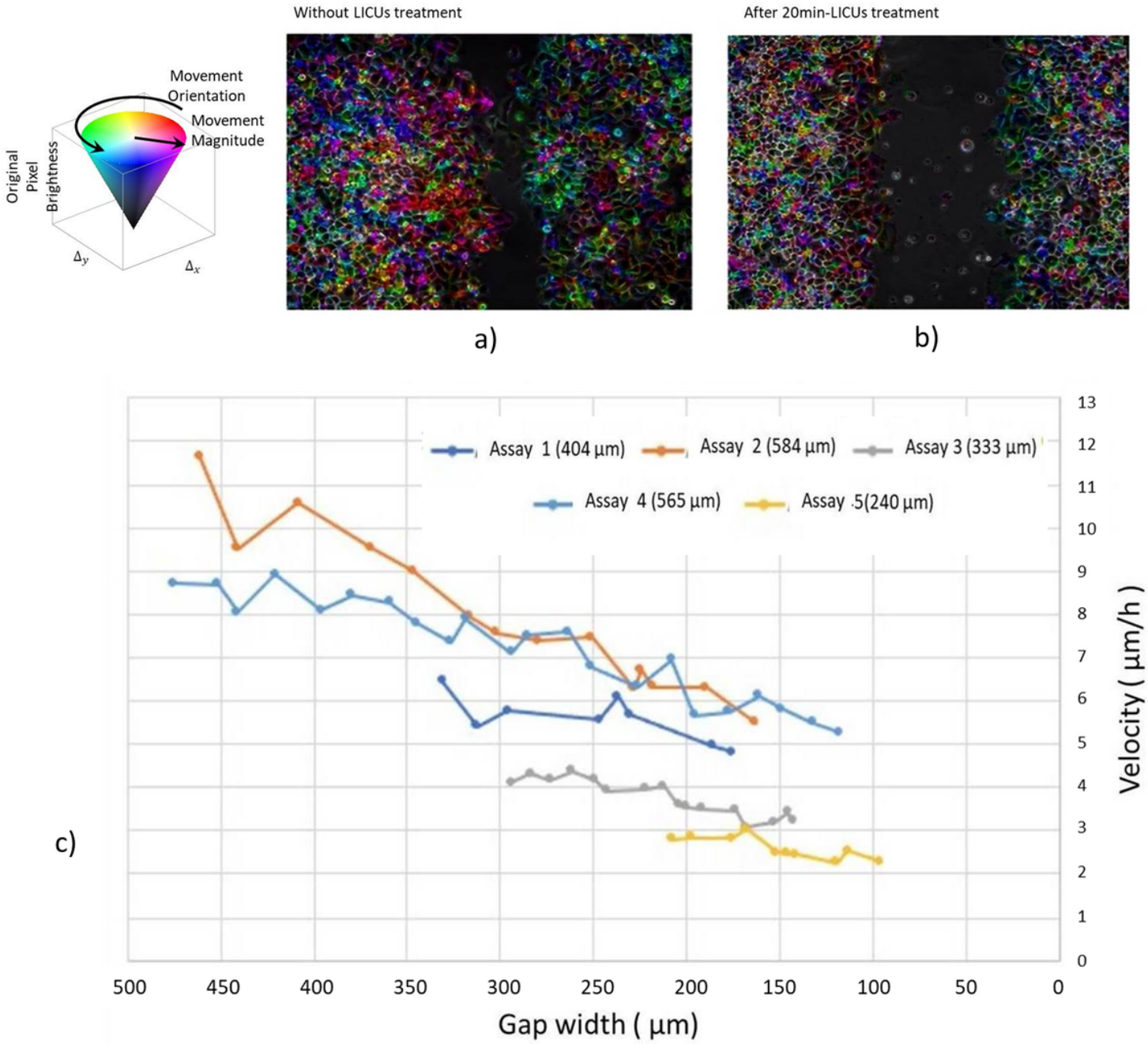

Figure 5

Colored cells during collective motion in a wound healing process a) without previous acoustic actuation and b) after 20 min of LICU irradiation prior to the sample culture process. Red refers to right-direction cell displacements,

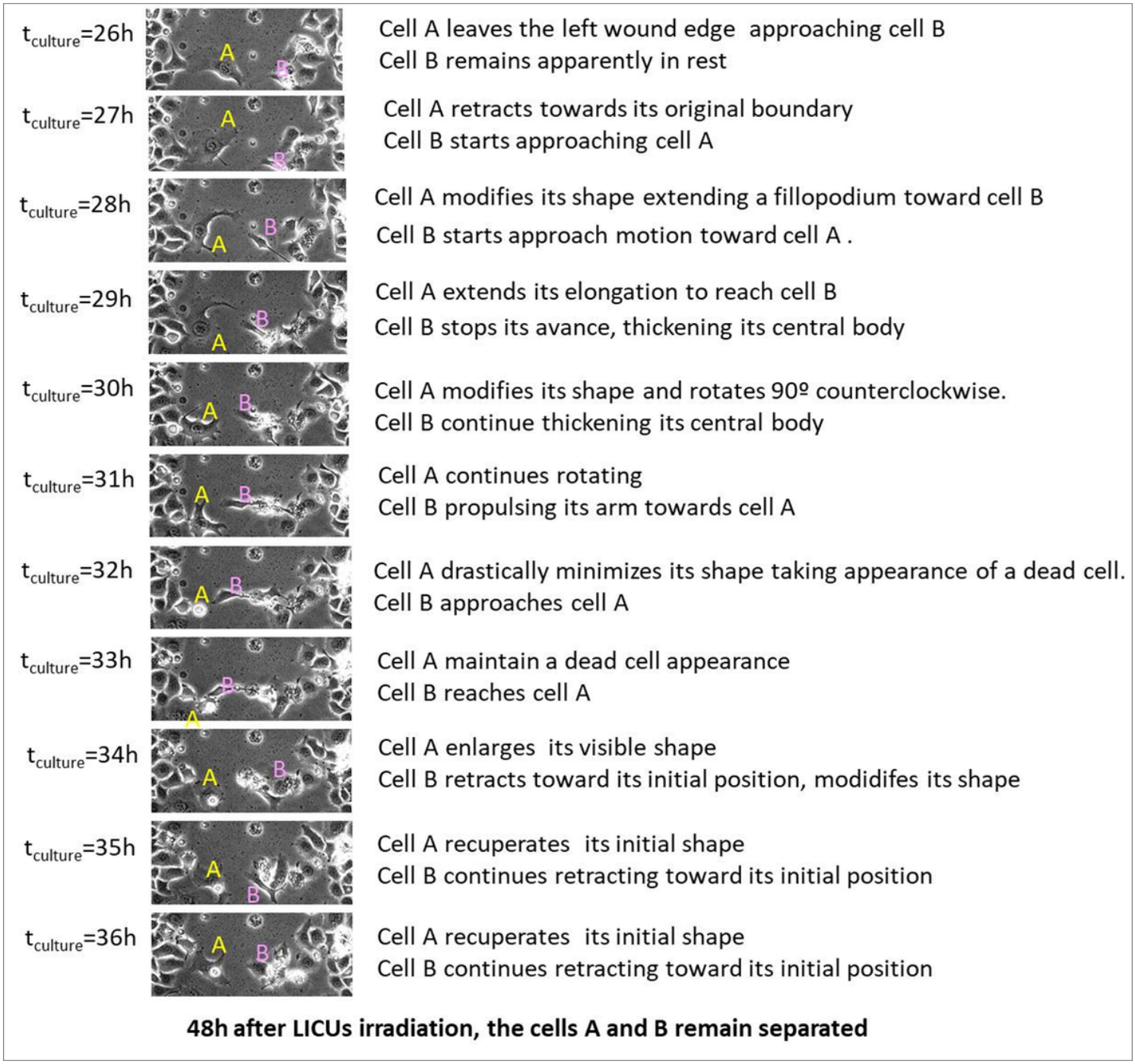

Figure 6

Detail of an attraction-repulsion process developed between two leader cells separated from the opposed boundaries of the wound during part of the 2nd day of culture that was previously irradiated with 20 min LICUs. After 48 hours, cells A and B remained separated, and both joined back to their respective initial wound boundaries.

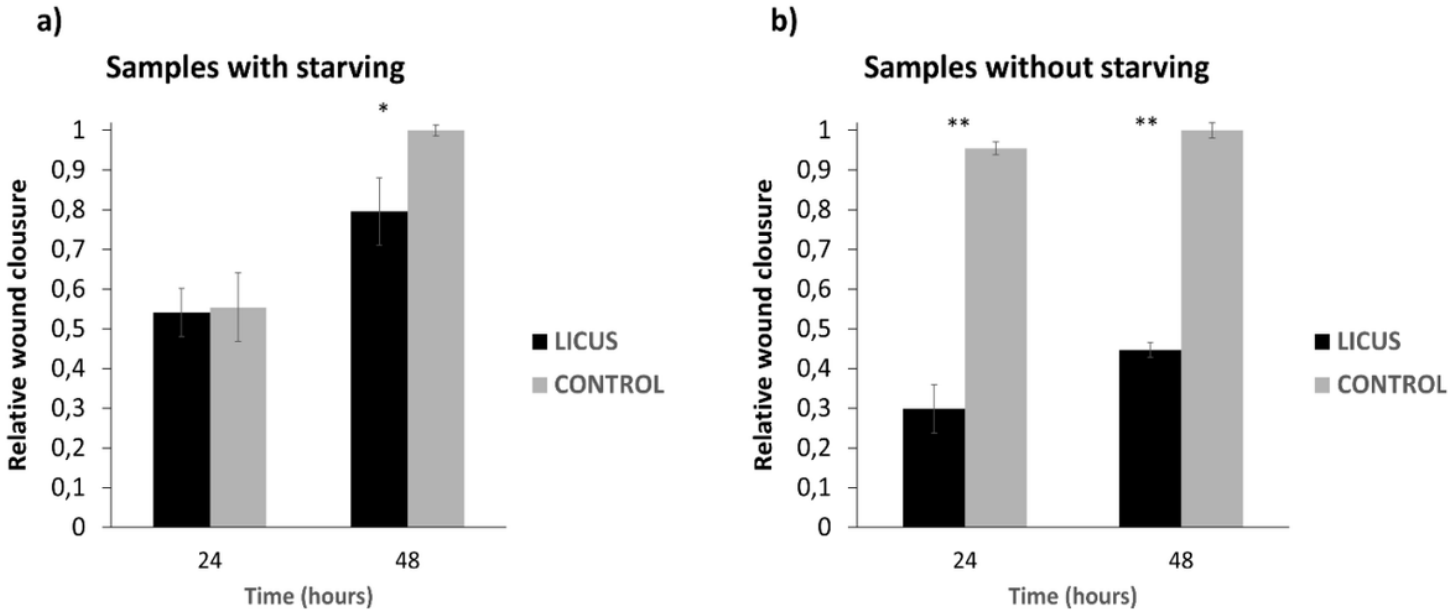

Figure 7

Quantification of relative wound closure under starving conditions and normal culture conditions of PANC-1 cells after 20 min of LICU actuation after 24 h and 48 h (n=3). Statistical significance *p≤0.05, **p≤0,01. U Mann-Whitney test.

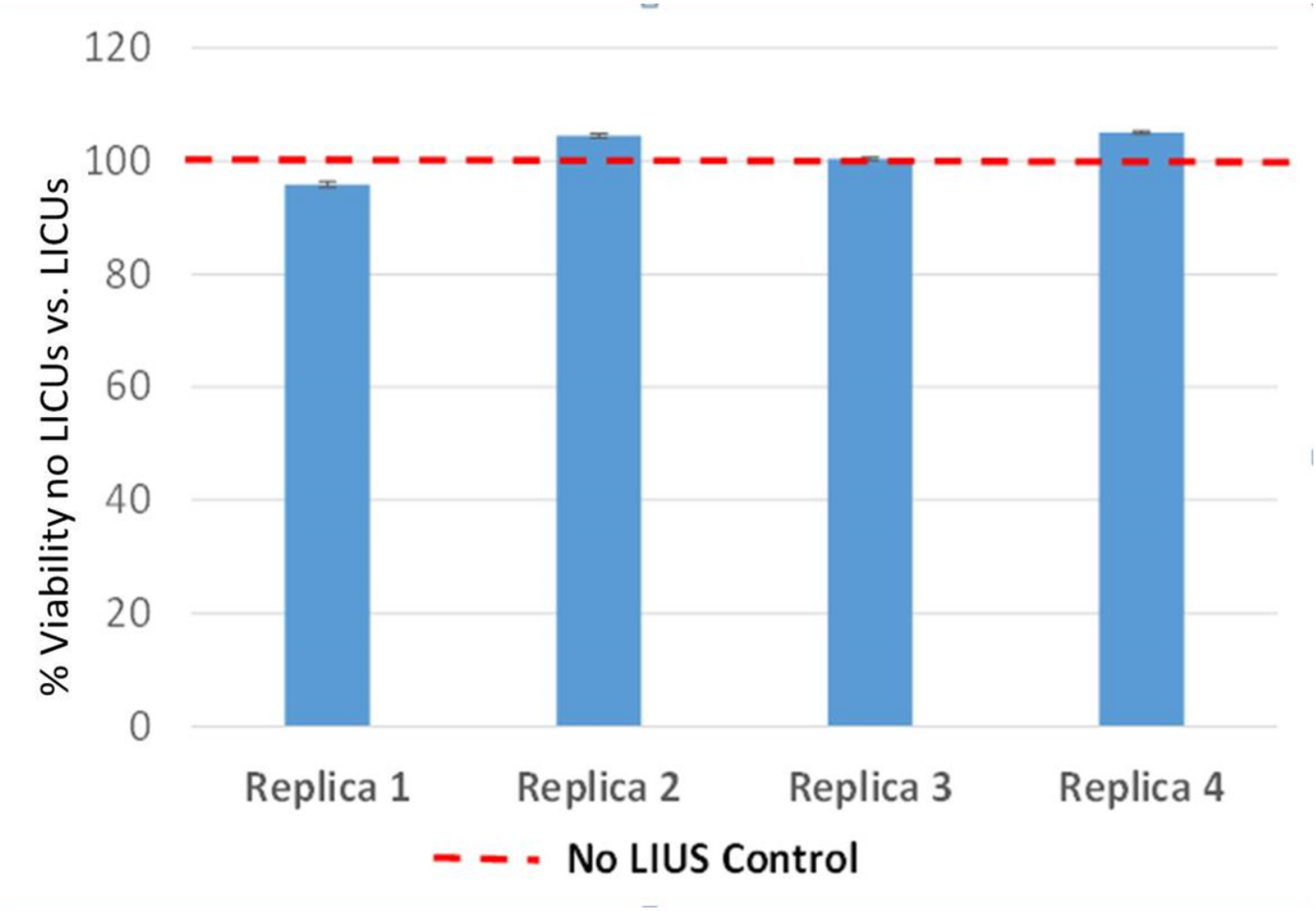

Figure 8

Analysis of cell viability after LICU treatment using Alamar BLUE assays performed in four replica experiments.

Supplementary Files

This is a list of supplementary files associated with this preprint. Click to download.

- MM1.mp4
- MM2.mp4